CIMAC CONGRESS 25
ZURICH, MAY 19 – 23, 2025

2025 | 088

Research on engine cylinder pressure identification method based on multi-signal fusion

Controls, Automation, Measurement, Monitoring & Predictive Maintenance

renqi Zhang, wuhan university of technology

yonghua Yu, wuhan university of technology
shunhua Ou, wuhan university of technology
lei Hu, wuhan university of technology
bingxin Cao, wuhan university of technology
bingjie Ma, national key laboratory of marine science and technology of china

DOI: https://doi.org/10.5281/zenodo.15259849

ABSTRACT

The cylinder pressure signal is one of the key indicators for evaluating the working process of an engine. Addressing the challenges faced in acquiring cylinder pressure signals due to the cost and inconvenience of installing cylinder pressure sensors for small or medium engines, an indirect measurement method of fusion easily measurable crankshaft torsional vibration and cylinder head vibration signals to identify cylinder pressure is proposed. After operating data were collected under different conditions through an engine test bench, the excitation and response characteristics of the crankshaft and connecting rod mechanism were analyzed combining these data with a multi-body dynamics model of the engine, and deep feature parameters of the crankshaft torsional vibration and cylinder head vibration signals were extracted. By integrating the physical information of the transmission characteristics of crankshaft torsional vibration and cylinder head vibration, and using machine learning algorithms, the cylinder pressure signal was identified. The identification accuracy under both normal and faulty engine states shows it can provide an effective reference for monitoring engine operating conditions.

1 INTRODUCTION

Direct measurement of cylinder pressure has many limitations in practical engineering applications. On the one hand, high-precision pressure sensors are expensive, especially when fully deployed in multi-cylinder engines, which significantly increases the overall cost; on the other hand, the installation of the sensors requires modification of the cylinder head, which will increase the design and manufacturing cost of the engine. In addition, the high temperatures and pressures inside the cylinders place severe demands on the durability of the sensors[1][2][3].

In response to the above problems, indirect measurement methods of cylinder pressure have gradually gained attention, i.e., identifying or reconstructing the pressure in the cylinder by acquiring signals that are easy to measure and have a low measurement cost. At present, scholars at home and abroad have proposed a variety of indirect measurement methods, mainly physical model method, signal analysis method, data-driven method and so on[4][5][6]. For example, based on the theoretical relationship between vibration velocity and cylinder pressure, Juan T et al.[7] derived the vibration characteristic parameter expression describing the peak pressure in the cylinder and verified the feasibility of the method. Huimin Z et al.[8] used VMD for noise reduction of vibration signals, trained 1D-CNN model to identify the cylinder pressure based on the noise reduced signals and cylinder pressure signals, and comparatively analysed the influence of the vibration signal measurement point location on the identification accuracy. Kim. G et al.[9] measured the vibration and in-cylinder pressure signals on a natural gas/diesel dual-fuel engine, constructed a deep neural network model for cylinder pressure reconstruction, and analysed in detail the influence of the main parameters on the prediction accuracy. Valencia-Duque A F et al.[10] proposed a time-delay neural networks (TDNN), which produced a stable cylinder pressure prediction performance by adjusting the delay of the TDNN based on the crankshaft speed in 12 engine operating states.

At present, there are some methods to indirectly measure the cylinder pressure of the engine, however, most of the existing methods are based on a single signal. Indirect measurement of cylinder pressure through a single signal has certain limitations, on the one hand, the engine in the actual operation of the working conditions are complex and variable, based on a single signal indirect measurement method is usually difficult to adapt to the diversity and variability of the working conditions. On the other hand, the single-signal method is more sensitive to abnormal signals, in practice, due to noise, transient interference and so on will cause signal anomalies, the single signal is easily affected by it, resulting in a large error in the measurement results[11][12]. Multi-signal fusion can effectively make up for the limitations of single-signal methods, improve the stability and accuracy of recognition through the comprehensive use of multi-source information, and has a strong fault tolerance. In recent years, multi-signal fusion technology has shown its excellent advantages in many fields such as fault diagnosis and pattern recognition. For example, Zejun Zheng et al.[13] constructed a fusion demodulation method that fuses the characteristic spectra of multi-channel signals and highlights the fault characteristic frequency, reflecting the superiority compared with other methods. Yan GH et al.[14] fused three-phase current and vibration signals using uses a three-column parallel CNN, then extracted features and identified faults according to BiLSTM, and the test results showed that the method was 4.2% more accurate than ordinary methods. Gai XY et al.[15] used Random Forest algorithm and KPCA algorithm to screen and reduce the dimensional fusion of multiple signal singularity features to establish the mapping relationship between the fused features and the degree of tool wear, which is used to identify the tool wear state, and the results show that the method can efficiently and accurately identify the wear state of the tool compared with some other methods. These studies have shown that multi-signal fusion techniques can make full use of the complementarity between different signals and exhibit high robustness and adaptability under complex working conditions. Based on this, this paper proposes a multi-signal fusion method for cylinder pressure identification, which fuses the signals of cylinder head vibration, crankshaft torsional vibration, and thermal parameters, and has a strong fault-tolerance capability while ensuring the accuracy of cylinder pressure identification.

The rest of the paper is as follows: section 2 describes the data acquisition and feature extraction, section 3 identifies the cylinder pressure, section 4 presents the results and discussion, and section 5 concludes the study.

2 DATA ACQUISITION AND FEATURE EXTRACTION

2.1 Data acquisition

The test object for CA4DLD type four-stroke diesel engine, doing work in the order of 1-3-4-2. A vibration sensors is installed on the 1st cylinder head to collect the cylinder head vibration signals during normal combustion of the diesel engine. Install a cylinder pressure sensor by drilling a hole in the cylinder head of the 1st cylinder to collect the pressure signal in the 1st cylinder. Install a

magnetoelectric sensor on the flywheel side to collect the torsional vibration signal of the crankshaft. Drill holes in the lubricating oil channel to install temperature sensors and pressure sensors to collect the lubricating oil temperature and pressure signals. A temperature sensor is punched and installed on the intake and exhaust manifolds to collect the intake and exhaust temperature signals. Other sensors are installed in a similar manner as above, with specific installation locations shown in Figure 1. The data acquisition platform uses NI CompactDAQ-9189, equipped with NI9231 vibration acquisition card to realise the dynamic acquisition of vibration signals, and NI9223 voltage acquisition card to realise the dynamic acquisition of cylinder pressure and top stop signals; The vibration sensor adopts BK4534B type sensor, the cylinder pressure sensor adopts Kistler 6052C31 type sensor; the upper stop sensor adopts SZB-16L type Hall sensor, and the temperature sensor adopts PT100 K type sensor.

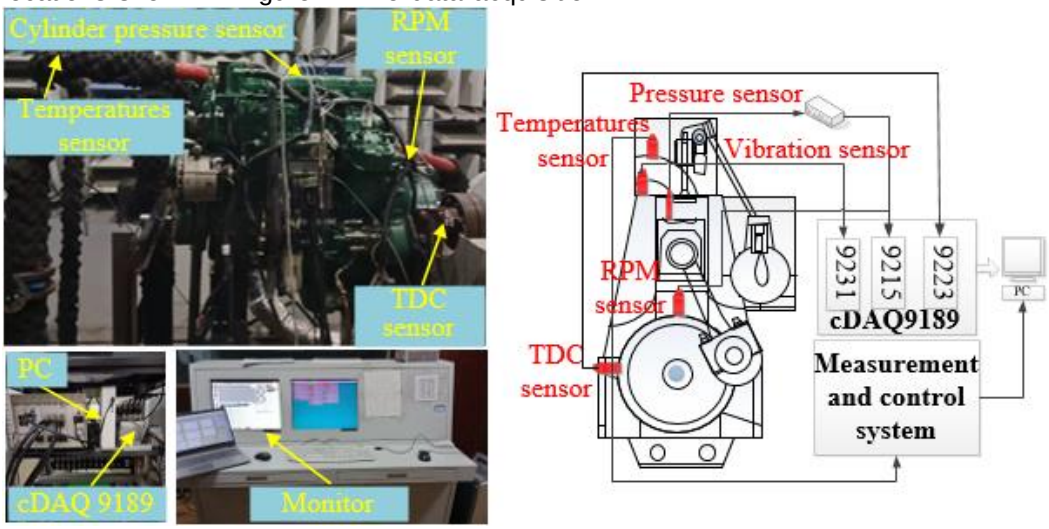

Figure 1. Schematic diagram of the test system

The engine was warmed up before data collection, and the data were collected after stabilisation. When the engine is running at 1200 r/min, the load is gradually increased in the order of 100N·m, 200N·m, 300N·m, 400N·m, 500N·m, 600N·m and 640N·m, and the signals of top dead center, cylinder head vibration, cylinder pressure and thermal parameters are collected simultaneously.

2.2 Feature extraction

In order to facilitate the systematic analysis and processing of the signals in each working cycle, the collected signals such as cylinder pressure and cylinder head vibration are intercepted for the whole cycle. Specifically, taking the piston movement to the compression top dead center position as the reference point, the crankshaft rotates one week between two adjacent compression top dead center, and a complete working cycle is carried out between three consecutive compression top dead center. According to this principle, the cylinder pressure, cylinder head vibration and other signals are intercepted for the whole cycle.

Calculate the distribution characteristics of the intercepted signal in the time domain, frequency domain and time-frequency domain, and obtain a series of key features that can reflect the operating state of the engine, which can effectively simplify the complexity of the signal data, and at the same time highlight and retain the most representative information in the signal. For the cylinder head vibration signal, 17 features were extracted in the time domain, including amplitude factor, root mean square and impact factor, etc.; and 4 features were extracted in the frequency domain, including centre of gravity frequency, mean square frequency band, etc. To further improve the feature discrimination accuracy, the extracted features are screened. According to the distinguishing ability of the features under different working conditions, the features with lower distinguishing degree are eliminated and the features with higher distinguishing degree are retained. After screening, 13 cylinder head vibration signal features with high discriminability are retained. The torsional vibration signals are processed in the same way as the thermal parameters.

3 CYLINDER PRESSURE IDENTIFICATION

3.1 Neural network mathematical model

In this study, Back Propagation Neural Network (BPNN) is used, BPNN has three main layers: input layer, hidden layer and output layer, the input layer is responsible for receiving the sample data, the

hidden layer is responsible for weighted summation of the sample data and nonlinear processing through the activation function, and the output layer is responsible for outputting the final result. BPNN contains three main steps in training: forward propagation, back propagation and iterative training[16][17].

Forward propagation means that the input layer receives the sample data and passes it to the hidden layer, where the neurons in the hidden layer perform a weighted summation of the sample data and output it after a nonlinear transformation through an activation function. The formula for the neuron is[18]:

$$y = \varphi\left(\sum_{i=1}^{n} \omega_i x_i + b\right) \qquad i = 0,1,2\cdots n \tag{1}$$

where x_i is the input of the ith neuron in the input layer, ω_i is the weight between neurons, b is the bias between neurons, and φ is the nonlinear activation function.

$$f\left(x_1, x_2, \cdots, x_n\right) \approx f\left(a_1, a_2, \cdots, a_n\right) + \sum_{i=1}^{n} \frac{\partial f}{\partial x_i}\left(a_1, a_2, \cdots, a_n\right) \bullet \left(x_i - a_i\right) \quad i = 0,1,2\cdots n \tag{2}$$

Order:

$$b = f\left(a_1, a_2, \cdots, a_n\right)$$
$$\sum_{i=1}^{n} \omega_i x_i = \sum_{i=1}^{n} \frac{\partial f}{\partial x_i}\left(a_1, a_2, \cdots, a_n\right) \bullet \left(x_i - a_i\right) \quad i = 0,1,2\cdots n \tag{3}$$

Then:

$$f\left(x_1, x_2, \cdots, x_n\right) \approx \sum_{i=1}^{n} \omega_i x_i + b \quad i = 0,1,2\cdots n \tag{4}$$

The first order Taylor expansion is a local linear approximation to the multivariate function $f(x_1,x_2...,x_n)$ at $(a_1,a_2...,a_n)$. From equations (1)~ (3), the work process of neuron can be equated to the local linear approximation of the multivariate function $f(x_1,x_2...,x_n)$ at $(a_1,a_2...,a_n)$.

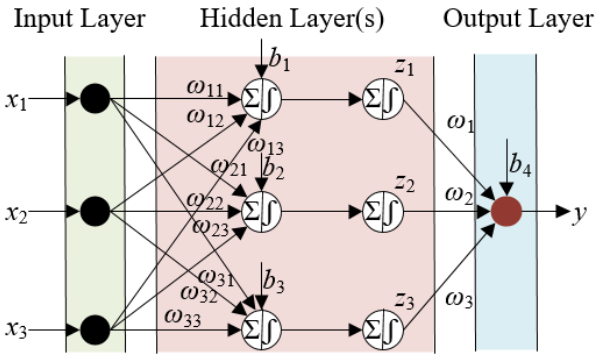

Figure 2. Schematic diagram of three-layer neural network structure

As shown in Figure 2, the corresponding equations in the three-layer neural network are:

$$\begin{aligned} z_1 &= \varphi\left(\omega_{11}x_1 + \omega_{12}x_2 + \omega_{13}x_3 + b_1\right) \\ z_2 &= \varphi\left(\omega_{21}x_1 + \omega_{22}x_2 + \omega_{23}x_3 + b_2\right) \\ z_3 &= \varphi\left(\omega_{31}x_1 + \omega_{32}x_2 + \omega_{33}x_3 + b_3\right) \\ y &= \omega_1 z_1 + \omega_2 z_2 + \omega_3 z_3 + b_4 \end{aligned} \tag{5}$$

In the forward propagation process, the initial values of ω and b ($\omega^{(0)}$, $b^{(0)}$) are first randomly selected, then the sample data are passed to each layer of the network for computation and generating the results, and finally the error values are computed by comparing the computed results with the actual values.

Backpropagation is based on the error value of each layer, using the gradient descent algorithm to solve for the local minima of the loss function, and constantly updating the weights and biases between neurons to achieve the minimum error between the output cylinder pressure curve and the measured cylinder pressure curve, i.e.

$$Minimize: E\left(\omega, b\right) = E_{(x,Y)}\left[\left(Y - y\right)^2\right] \tag{6}$$

$E(x,Y)$ is the mathematical expectation of the traversed training samples, Y is the measured value and y is the neural network model output value.

The gradient descent algorithm used in BPNN is Levenberg-Marquardt (L-M) algorithm, which is a small batch gradient descent algorithm, i.e., the entire sample set is divided into batches, and the first batch of samples is forward propagated during training to calculate its average error. Then forward propagate the samples of the second batch, calculate its average error, and so on until all the

samples of the batch have been processed by the network, and output the average error value of the current round.

The objective function is assumed to be a one-dimensional function $f(x)$, as shown in Figure 3:

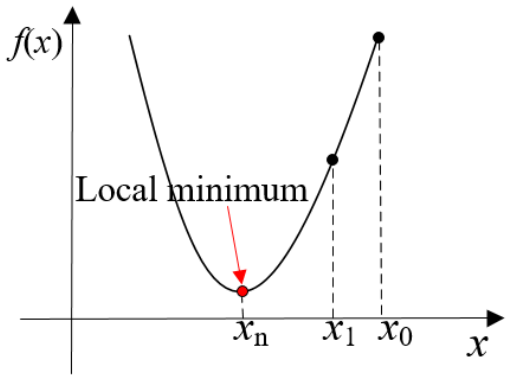

Figure 3. Objective function $f(x)$

Calculate the gradient at position x_0 and move one small step in the direction of the negative value of the gradient to get x_1, i.e.

$$x_1 = x_0 - \alpha \left.\frac{df}{dx}\right|_{x_0} \tag{7}$$

According to Taylor's formula:

$$\begin{aligned} f(x_1) &= f\left(x_0 - \left.\frac{df}{dx}\right|_{x_0}\right) \\ &= f(x_0) + \left.\frac{df}{dx}\right|_{x_0}\left[-\left.\frac{df}{dx}\right|_{x_0}\right] + o(\Delta x) \\ &= f(x_0) - \alpha\left[-\left.\frac{df}{dx}\right|_{x_0}\right]^2 + o(\Delta x) \end{aligned} \tag{8}$$

α is the learning rate. It can be seen that $f(x_1) < f(x_0)$, and the iterations are carried out sequentially until the point where the local minima of the objective function $f'(x_n) = 0$ is found.

The update equations for ω and b are:

$$\begin{aligned} \omega^{(n+1)} &= \omega^{(n)} - \alpha \left.\frac{\partial E}{\partial \omega}\right|_{\left(\omega^{(n)}, b^{(n)}\right)} \\ b^{(n+1)} &= b^{(n)} - \alpha \left.\frac{\partial E}{\partial b}\right|_{\left(\omega^{(n)}, b^{(n)}\right)} \end{aligned} \tag{9}$$

The Taylor expansion of $E(\omega,b)$ is:

$$\begin{aligned} E(\omega_0 + \Delta\omega, b_0 + \Delta b) &= E(\omega_0, b_0) + \\ \left.\frac{\partial E}{\partial \omega}\right|_{(\omega_0, b_0)} \Delta\omega + \left.\frac{\partial E}{\partial b}\right|_{(\omega_0, b_0)} \Delta b + o\left(\sqrt{\omega_0^2 + b_0^2}\right) \end{aligned} \tag{10}$$

Substituting equation (9) into (10) and simplifying gives:

$$\begin{aligned} E\left(\omega^{(n+1)}, b^{(n+1)}\right) &= E\left(\omega^{(n)}, b^{(n)}\right) - \alpha\left[\left.\frac{\partial E}{\partial \omega}\right|_{\left(\omega^{(n)}, b^{(n)}\right)}\right]^2 \\ &- \left[\left.\frac{\partial E}{\partial b}\right|_{\left(\omega^{(n)}, b^{(n)}\right)}\right]^2 + o\left(\sqrt{\omega_0^2 + b_0^2}\right) \end{aligned} \tag{11}$$

If $\partial E/\partial\omega$, $\partial E/\partial b$ are not all zero on $(\omega^{(n)},b^{(n)})$, then there must be $E(\omega^{(n+1)},b^{(n+1)}) < E(\omega^{(n)},b^{(n)})$.

The partial derivatives that need to be solved in the process of solving for the extremes of the objective function by the gradient descent method are, respectively:

$$\left(\frac{\partial E}{\partial \omega_{11}}, \cdots, \frac{\partial E}{\partial \omega_{31}}, \frac{\partial E}{\partial \omega_1}, \cdots, \frac{\partial E}{\partial \omega_3}, \frac{\partial E}{\partial b_1}, \cdots, \frac{\partial E}{\partial b_4}\right) \tag{12}$$

From equation (6), we can see that

$$\frac{\partial E}{\partial y} = y - Y \tag{13}$$

Using the known partial derivatives to solve for the unknown partial derivatives according to the chain derivation rule, we get

$$\frac{\partial E}{\partial a_1}=\frac{\partial E}{\partial y}\bullet\frac{\partial y}{\partial a_1}\Rightarrow\frac{\partial E}{\partial a_1}=\frac{\partial E}{\partial y}\bullet\frac{\partial y}{\partial z_1}\bullet\frac{\partial z_1}{\partial a_1}\Rightarrow$$
$$\frac{\partial E}{\partial a_1}=\omega_1\left(y-Y\right)\varphi'\left(a_1\right) \quad (14)$$

The updating of ω and b can be done by substituting it into the updating equation for ω and b.

Iterative training is the process of continuously performing forward and back propagation to update ω and b until the error is minimized.

3.2 Training results

Sample sets at 1200r/min, 100N·m, 200N·m, 300N·m, 400N·m, 500N·m, 600N·m and 640N·m under seven operating conditions were formed through feature extraction and screening, with 30 samples under each operating condition, each of which includes: 13 cylinder head vibration signal combustion segment features, 11 torsional vibration signal features, 16 thermal parameters, while a total of 200 points in the cylinder pressure signal combustion section (300°CA~420°CA) are extracted as labels corresponding to each sample. The size of the feature matrix is 210×40 and the size of the cylinder pressure matrix is 210×200. 80% of them were used as training dataset for neural network model training and 20% as validation dataset to verify the performance of the network model.

The parameters of BPNN are set as follows: the number of network layers is 3, the number of neurons in the hidden layer is 10, the learning rate is 0.001, the activation function is tanh(x), the training algorithm is L-M, and the convergence criterion is the early stopping method.

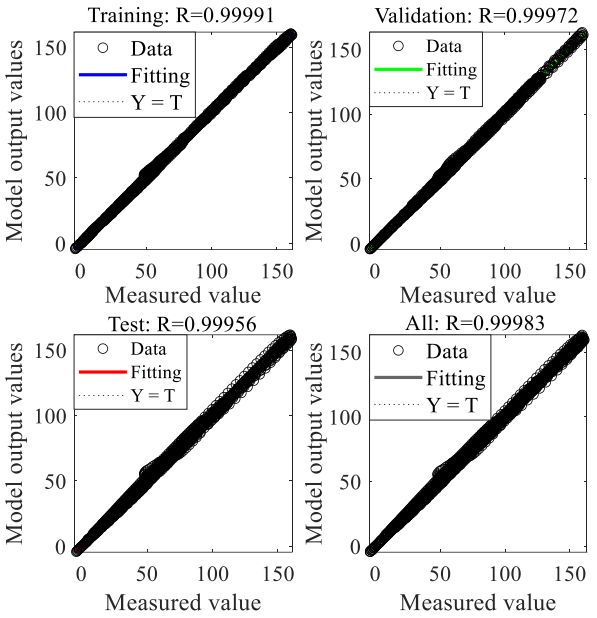

Figure 4. Regression plot of BPNN model

The regression plot shown in Figure 4 demonstrates the linear relationship between the output values of the network model and the true values and the effect of the fit, reflecting the identification accuracy of the model. The diagonal line is the fitted line in the ideal state, indicating the case where the output value of the network model is exactly equal to the true value. As shown in Figure 6, the data points are centrally distributed near the diagonal line, indicating that the error between the model output value and the true value is small. The correlation coefficient R is 0.99, indicating a strong linear relationship between the output values and the true values, and the model has a high recognition accuracy.

4 RESULTS AND DISCUSSION

4.1 Identification results

In order to evaluate the accuracy of the multi-signal fusion-trained neural network model in recognising cylinder pressure, the peak pressure and its location are used as evaluation indexes. The peak value is an important parameter to measure the recognition result in terms of amplitude accuracy; the peak pressure location is the crank angle when the peak pressure appears, which is used to assess the recognition accuracy of the recognition result in terms of timing. These two indicators can comprehensively reflect the amplitude and phase errors in cylinder pressure recognition, thus providing a quantitative basis for evaluating the recognition effect of the neural network model. The recognition results of the network model trained by multi-signal fusion are shown in Figure 5.

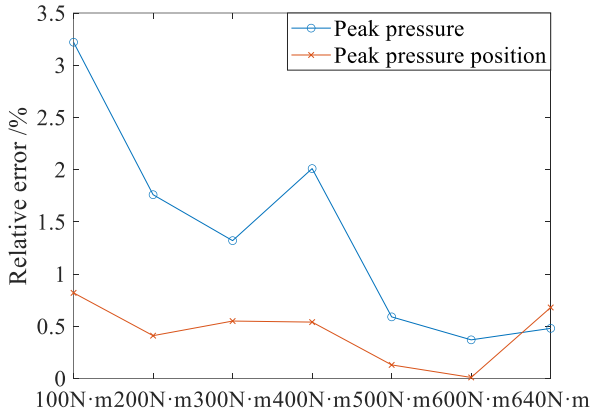

Figure 5. Comparison of relative error between identified cylinder pressure and measured cylinder pressure

As can be seen from Figure 5, the BPNN model shows high accuracy in identifying the cylinder pressure under different operating conditions, with the maximum value of the average relative error being 3.22% and the minimum value being 0.01%. It is worth noting that the network model used is not an independent model trained separately for each operating condition, but a single network model trained based on the fusion of signal data from multiple operating conditions. The model is able to output stable and accurate cylinder pressure curves even when the operating conditions change, which indicates that the network model with multiple signal fusion has strong cross-condition adaptability and generalisation ability, and avoids the need to train the model individually for each condition, which improves the training efficiency and practicability of the model.

4.2 Fault-tolerant performance analysis of multi-signal fusion

In practical application environments, a single sensor may fail or be affected by external interference, resulting in signal loss or distortion, thus limiting the accuracy of cylinder pressure recognition. Through the multi-signal fusion strategy, even if one sensor fails or the signal is invalid, the cylinder pressure recognition can still be maintained with high accuracy by the data information provided by other sensors, which enhances the robustness and reliability of the model under the fault state. Therefore, the fault-tolerance performance of the multi-signal fusion strategy is further analysed to verify the recognition accuracy and stability of the model under a sensor failure scenario.

There is an important correlation between exhaust temperature and cylinder pressure. During engine operation, the cylinder pressure, as a key characterisation of the combustion process, directly reflects the combustion state of the gas mixture in the cylinder and its thermodynamic properties. The fluctuation of exhaust gas temperature is usually caused by the changes of heat release and energy conversion efficiency during the combustion process, therefore, the exhaust gas temperature is usually regarded as an indirect characterisation of the cylinder pressure change. Based on this, the failure of the exhaust gas temperature sensor is analysed as an example to verify the fault-tolerance performance of the multi-signal fusion strategy.

Common manifestations of exhaust temperature sensor failure include the following three situations: first, the collected signal value is significantly lower than the normal state value, second, the collected signal value is significantly higher than the normal state value, and third, there are abnormal fluctuations in a certain period of time. This is due to the sensor in the acquisition of the signal process due to the sensing element damage, performance decline or external interference caused by the output temperature value deviation from the normal range, as shown in Figure 6.

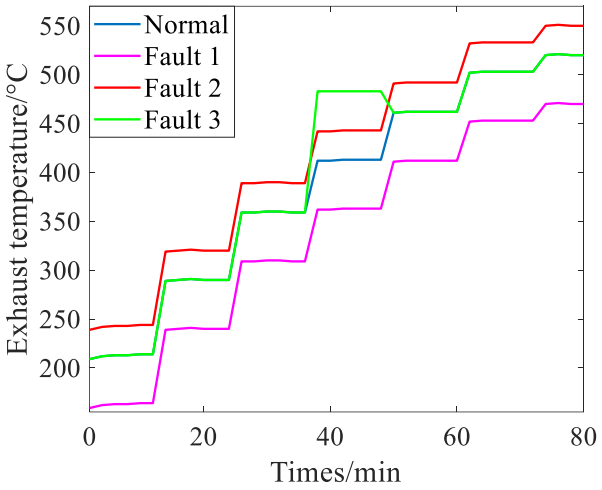

Figure 6. Comparison of relative error between identified cylinder pressure and measured cylinder pressure

The samples in the faulty state are input into the model trained using the data in the normal state, the corresponding cylinder pressure signals are identified, and the average relative error between the pressure maximum and the location of the pressure maximum is used as the evaluation index of the model performance, and the results are shown in Figure 7.

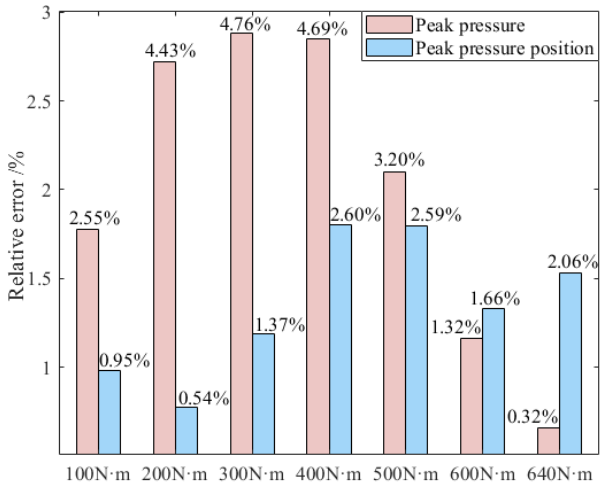

(a)

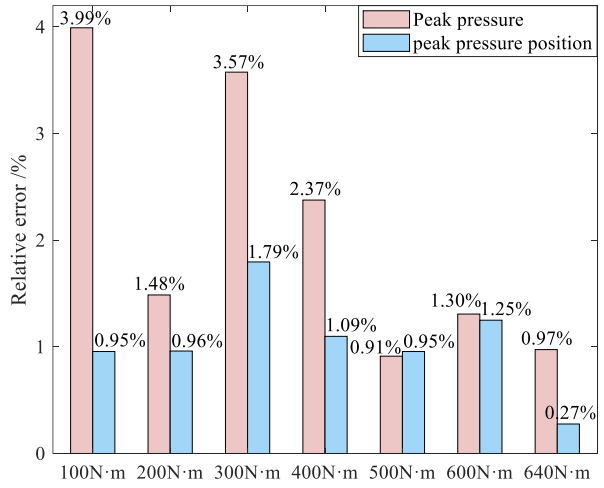

(b)

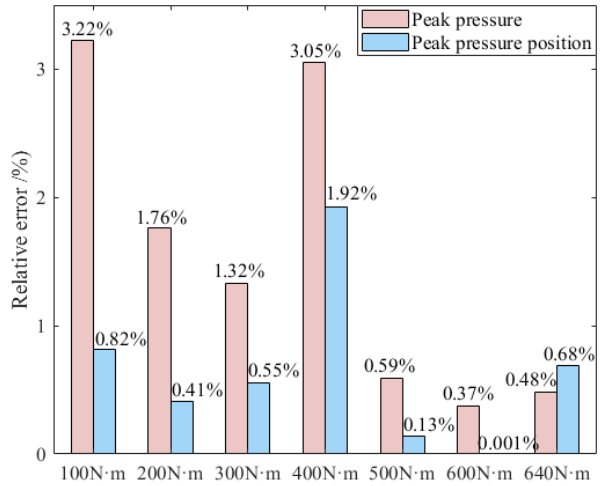

(c)

Figure 7. Comparison of the relative error between the recognised cylinder pressure and the measured cylinder pressure: (a) Fault type 1: Exhaust gas temperature sensor signal value is lower than the normal state. (b) Fault type 2: Exhaust gas temperature sensor signal value is higher than normal. (c) Fault type 3: The exhaust temperature sensor signal value fluctuates abnormally during a certain period of time.

As can be seen in Figure 7, the neural network model with multi-source information fusion shows excellent fault tolerance performance in cylinder pressure recognition under three different fault types. Under the three fault types of low, high and abnormal fluctuations of the sensor acquisition signal, the model is still able to control the average relative error of the maximum value of the cylinder pressure and its location within 5%, which indicates that the model has a strong anti-interference ability to a sensor abnormality. The multi-source information fusion strategy compensates for the lack of fault signals with data from other sensors, so that the recognition accuracy is still maintained under individual sensor fault conditions. This fault tolerance not only enhances the robustness of the model, but also improves its reliability in complex application environments and ensures the stability of cylinder pressure recognition under multiple load and sensor fault conditions.

5 CONCLUSIONS

The multi-source information fusion strategy has high cylinder pressure recognition accuracy and stability. By fusing multiple signals such as cylinder head vibration, crankshaft torsion vibration, and thermal parameters, it can capture the running state of the engine more comprehensively and accurately, so as to ensure the recognition accuracy of the cylinder pressure, in which the average relative error of the peak pressure and the average relative error of the location of the peak pressure are 1.39% and 0.44%, respectively.

The method of multi-source information fusion has good fault tolerance. When individual sensors fail, a high recognition accuracy can still be ensured. Specifically, when different types of faults occur in individual sensors, the average relative errors of the identified pressure maxima and the location of the pressure maxima are less than 5%, which demonstrates the good accuracy and reliability of the method in practical applications, lays a technical foundation for the development of an engine health monitoring system under complex operating conditions, and makes it possible to sense the engine state based on multi-source information fusion. The scope of future work applies the method to the intelligent operation and maintenance of engines.

6 DEFINITIONS ACRONYMS, ABBREVIA

TIONS

VMD	The variational mode decomposition
CNN	The convolutional neural network
BiLSTM	Bi-directional long short-term memory
KPCA	Kernel principal component analysis
TDNN	The time-delay neural network
BPNN	The back propagation network
X_i	The input of the ith neuron in the input layer
ω_i	The weights between neurons
b	The bias between neurons
φ	The nonlinear activation function
E	The mathematical expectation
Y	The measured value
y	The neural network model output value

7 ACKNOWLEDGMEENTS

Thanks to the funding and support of the National Natural Science Foundation of China (No.52271328), this research is also supported by the National Key Laboratory of Marine Engine Science and Technology of China (No.LAB-2023-02).

8 REFERENCES AND BIBLIOGRAPHY

[1] D.T. Hountalas, R.G. Papagiannakis, G. Zovanos, et al., 2014. Comparative evaluation of various methodologies to account for the effect of load variation during cylinder pressure measurement of large scale two-stroke diesel engines, *Applied Energy*, 113:1027–1042.

[2] A.T. Doppalapudi, A.K. Azad. 2014. Advanced numerical analysis of in-cylinder combustion and NOx formation using different chamber geometries. *Fire*. 7(2): 35.

[3] S. A. Malan, L. Ventura, A. Manelli. 2021. Cycle to cycle closed-loop combustion control through virtual sensor in a diesel engine, *Mediterranean Conference on Control and Automation*. 1179–1184.

[4] Z. Renqi, Y. Yonghua, O. Shunhua, et al., 2025. Research on the identification method of peak pressure by fusion of time-domain averaging and transfer function, *Measurement*, 242:116090.

[5] V.C. Mariani, S. H. Och, L.D.S. Coelho, et al., 2019. Pressure prediction of a spark ignition single cylinder engine using optimized extreme learning machine models, *Applied Energy*. 249: 204-221.

[6] O. Shunhua, Y. Yonghua, Y. Jianguo. 2022. Identification and reconstruction of anomalous sensing data for combustion analysis of marine diesel engines, *Measurement*, 193:110960.

[7] T Juan, HU Yunping, WEI Qingtan, et al, 2019. Extraction method of in-cylinder peak pressure based on vibration velocity of diesel engine, *Vehicle engine*, 4: 88-92.

[8] Z Huimin, WANG Shuangpeng, MEI Jianmin, et al, 2022. Cylinder pressure identification based on VMD and one-dimensional convolutional neural network, *Journal of military transportation: equipment & technology*, 3:32-37.

[9] Kim. G, Park. C, Kim. W,. et al., 2023. The effect of engine parameters on in-cylinder pressure reconstruction from vibration signals based on a DNN model in CNG-diesel dual-fuel engine, *SAE Technical Paper*.

[10] Valencia-Duque AF, Cárdenas-Peña DA, Álvarez-Meza AM, et al. 2021. Tdnn-based engine in-cylinder pressure estimation from shaft velocity spectral representation. *Sensors*. 21(6):2186.

[11] Serkan, Kulah, Alexandru, et al., 2018. Robust cylinder pressure estimation in heavy-duty diesel engines. *International Journal of Engine Research*, 19:179-188.

[12] S. Polat, O. Özdilli, H. Çizmeci, et al., 2019. An estimation of in-cylinder pressure based on lambda and engine speed in hcci engine using artificial neural networks. *Fresenius Environmental Bulletin.* 28: 3568-3576.

[13] Zejun Zheng, Dongli Song, Weihua Zhang, et al, 2025. A fault diagnosis method for bogie axle box bearing based on sound-vibration multiple signal fusion, *Applied Acoustics*, 228:110336.

[14] Yan, Guohua & Hu, Yihuai. 2024. Inter-turn short circuit and demagnetization fault diagnosis of ship PMSM based on multiscale residual dilated CNN and BiLSTM. *Measurement Science and Technology*. 35.

[15] Gai, X., Cheng, Y., Guan, R. et al. 2022. Tool wear state recognition based on WOA-SVM with statistical feature fusion of multi-signal singularity. *Int J Adv Manuf Technol*, 123: 2209–2225.

[16] Foukalas, F. 2025. A survey of artificial neural network computing systems. *Cogn Comput,*17:4.

[17] M. Raissi, P. Perdikaris, G.E. Karniadakis, 2017. Physics informed deep learning (Part I): data-driven solutions of nonlinear partial differential equations.

[18] S. Cuomo, V.S.D. Cola, F. Giampaolo, et al., 2022. Scientific machine learning through physics-informed neural networks: where we are and what's next, *Journal of Scientific Computing*, 92(3):6-67.

9 CONTACT

Renqi Zhang

Wuhan University of Technology

E-mail: 349043@whut.edu.cn

Yonghua Yu

Wuhan University of Technology

E-mail: yyhua@whut.edu.cn

Shunhua Ou

Wuhan University of Technology

E-mail: oushunhua2021@163.com

Lei Hu

Wuhan University of Technology

E-mail: hulei_nd@whut.edu.cn

Bingxin Cao

Wuhan University of Technology

E-mail: bxcao@whut.edu.cn

Bingjie Ma

National Key Laboratory of Marine Engine Scienceand Technology of China

E-mail: oscejie@163.com